



**University of
Zurich**^{UZH}

**Zurich Open Repository and
Archive**

University of Zurich
University Library
Strickhofstrasse 39
CH-8057 Zurich
www.zora.uzh.ch

Year: 2018

A non-equilibrium approach to allosteric communication

Stock, Gerhard ; Hamm, Peter

Abstract: While the theory of protein folding is well developed, including concepts such as rugged energy landscape, folding funnel, etc., the same degree of understanding has not been reached for the description of the dynamics of allosteric transitions in proteins. This is not only due to the small size of the structural change upon ligand binding to an allosteric site, but also due to challenges in designing experiments that directly observe such an allosteric transition. On the basis of recent pump-probe-type experiments (Buchli et al. 2013 Proc. Natl Acad. Sci. USA110, 11 725–11 730. (doi:10.1073/pnas.1306323110)) and non-equilibrium molecular dynamics simulations (Buchenberg et al. 2017 Proc. Natl Acad. Sci. USA114, E6804–E6811. (doi:10.1073/pnas.1707694114)) studying an photoswitchable PDZ2 domain as model for an allosteric transition, we outline in this perspective how such a description of allosteric communication might look. That is, calculating the dynamical content of both experiment and simulation (which agree remarkably well with each other), we find that allosteric communication shares some properties with downhill folding, except that it is an ‘order–order’ transition. Discussing the multiscale and hierarchical features of the dynamics, the validity of linear response theory as well as the meaning of ‘allosteric pathways’, we conclude that non-equilibrium experiments and simulations are a promising way to study dynamical aspects of allostery.

DOI: <https://doi.org/10.1098/rstb.2017.0187>

Posted at the Zurich Open Repository and Archive, University of Zurich

ZORA URL: <https://doi.org/10.5167/uzh-173928>

Journal Article

Accepted Version

Originally published at:

Stock, Gerhard; Hamm, Peter (2018). A non-equilibrium approach to allosteric communication. *Philosophical Transactions of the Royal Society of London. Series B: Biological Sciences*, 373(1749):20170187.

DOI: <https://doi.org/10.1098/rstb.2017.0187>

A Nonequilibrium Approach to Allosteric Communication

Gerhard Stock

Biomolecular Dynamics, Institute of Physics, Albert Ludwigs University, Freiburg, Germany

Peter Hamm

Department of Chemistry, University of Zurich, Zurich, Switzerland

(Dated: July 15, 2019)

While the theory of protein folding is well developed, including concepts such as rugged energy landscape, folding funnel, etc., the same degree of understanding has not been reached for the description of the dynamics of allosteric transitions in proteins. This is in part due to the small size of the structural change upon ligand binding to an allosteric site, but also due to challenges in designing experiments that directly observe such an allosteric transition. On the basis of recent pump-probe-type experiments (Proc. Natl. Acad. Sci. 110, 11725 (2013)) and nonequilibrium molecular dynamics simulations (Proc. Natl. Acad. Sci. 114, E6804 (2017)) studying an photoswitchable PDZ2 domain as model for an allosteric transition, we outline in this Perspective how such a description of allosteric communication might look like. That is, calculating the dynamical content of both experiment and simulation (which agree remarkably well with each other), we find that allosteric communication shares some properties with downhill folding, except that it is an “order-order” transition. Discussing the multiscale and hierarchical features of the dynamics, the validity of linear response theory as well as the meaning of “allosteric pathways”, we conclude that nonequilibrium experiments and simulations are a promising way to study dynamical aspects of allostery.

I. INTRODUCTION

Describing the puzzling phenomenon of long-range communication between distant protein sites, allostery has been intensively studied in experiment and computation [1–9]. In spite of its importance as elementary process of cell signaling as well as target in pharmaceutical research, there is surprisingly little known about the underlying *dynamical process* of allosteric communication. Most commonly, allostery is related to the binding of a ligand to the allosteric site, which triggers the conformational change at a distant site of the protein. This so-called “allosteric transition”, however, has been rarely observed directly, in part because of the smallness of the structural changes, the experimental challenges to observe transition pathways and also because the timescale limitations of molecular dynamics (MD) simulations [10–14]. This situation is in striking variance to the protein folding problem, where several decades of theoretical and experimental work have resulted in a quite well-established picture how folding and unfolding proceed [15]. This includes general scenarios such as two-state and downhill folding [16, 17], dynamical mechanisms such as zipping or diffusion limited processes [15], as well as a wealth of theoretical formulations, including the concepts of rugged energy landscapes and folding funnel [18, 19] or Markov state models [20]. In comparison, a dynamical picture of the allosteric transition appears to be still in its infancy.

With “dynamics”, we here do *not* refer to the rates of ligand binding and unbinding, k_{on} and k_{off} , respectively. These rates represent very well established concepts in biochemistry, as their ratio is related to the binding free energy via $k_{\text{on}}/k_{\text{off}} = e^{-\Delta G/k_B T}$. With “dynamics”, we also do not mean equilibrium fluctuations, which are dis-

cussed as another possible mechanism of allostery with essentially no structural changes [21, 22]. Rather, with “dynamics” we refer to the nonequilibrium response that transfers a signal within an allosteric protein, triggered by ligand binding or unbinding. However, most experiments and theories of allostery have focused on equilibrium systems, i.e., the starting and end states of an allosteric transition, hence they cannot say much about possible intermediates.

The direct observation of nonequilibrium processes in an allosteric protein requires us to define a starting point (say, time $t = 0$) and a time-dependent observable describing the progress of the process. These requirements are naturally provided in a pump-probe-type experiment, in which an allosteric transition is triggered by light on a timescale that is fast compared to any biologically relevant timescale. In the realm of femtochemistry [23], that makes the difference between “kinetics”, which in essence is an equilibrium concept (since $k_{\text{on}}/k_{\text{off}} = e^{-\Delta G/k_B T}$), and nonequilibrium “dynamics”. Designing photoswitchable proteins is one possible approach to achieve a phototriggerable system (besides temperature- [24, 25] and pH-jumps [26, 27]), which has already been applied to the protein folding problem [28–30]. In the context of allostery, this approach was recently demonstrated experimentally by Buchli et al. [31] and computationally by Buchenberg et al. [32] for a PDZ2 domain.

PDZ domains have been studied extensively as model systems for allosteric communication [33–36]. They represent an important class of protein interaction modules that are involved in the regulation of multiple receptor-coupled signal transduction processes. They share a common fold, which consists of two α -helices and six β -strands, with the second α -helix and the second β -strand forming the canonical binding groove (Fig. 1), and gen-

erally bind the C-terminus of their targets. One particularly illustrative example is the PDZ3 domain from PSD-95, which has a short additional third α -helix at the C-terminus. It has been shown that the removal of that helix, or its unfolding upon phosphorylation, significantly reduces the ligand binding affinity [34]. Here, we focus on the simpler PDZ2 domain from human tyrosine-phosphatase 1E (hPTP1E), which lacks that additional α -helix, but which has been demonstrated to possess allosteric properties as well [33], albeit not in the sense of functional allostery between two ligands. Both the PDZ2 and the PDZ3 domain have been studied in particular with regard to intramolecular signaling pathways [37–42], but the nature of the allosteric interaction remains a matter of debate. While they are discussed as examples for a modulated side-chain dynamics being responsible for the allosteric mechanism [33, 34, 43, 44], ligand binding to the PFZ2 domain also results in a small but measurable structural change of about 0.5 Å RMSD [45].

To explore in real time how such a structural change propagates through the protein, Buchli et al.[31] have covalently linked an azobenzene photoswitch across the binding groove of PDZ2 and used an ultrafast laser pulse that effects *cis*→*trans* photoisomerization of azobenzene. This results in a photoinduced opening of the binding pocket, which structurally mimics the apo-to-ligand-bound transition of native PDZ2 (Fig. 1). The latter has been verified with the help of NMR structure analysis of the starting and end point of the photoinduced transition [31], that is structurally very similar to the apo and ligand-bound structure of native PDZ2 [45]. Employing ultrafast time-resolved vibrational spectroscopy, they showed that the conformational rearrangement of the photoswitchable protein occurs on various timescales from pico- to microseconds in a highly non-exponential manner. The subsequent detailed MD study of the nonequilibrium dynamics by Buchenberg et al.[32] reproduced many of these finding and revealed a microscopic picture of the process.

Based on these experimental and computational works, in this Perspective we want to outline a time-dependent nonequilibrium description of the dynamical process of allostery. Employing a time scale analysis to reveal the “dynamical content” [46–50] of the spectroscopic time traces as well as of the computed intramolecular $C\alpha$ -distances of the protein, we investigate the origin of the nonexponential kinetics and overshootings exhibited by these observables. In particular, we identify three physically distinct phases of the time evolution, describing elastic response ($\lesssim 0.1$ ns), inelastic reorganization (~ 100 ns) and structural relaxation ($\gtrsim 1\mu$ s), and explain the dynamics in terms of the free energy landscape of the allosteric transition. Issues such as the similarity to the “strange kinetics” observed in downhill folding [51, 52] as well as the interpretation of allosteric pathways [5, 53] are discussed.

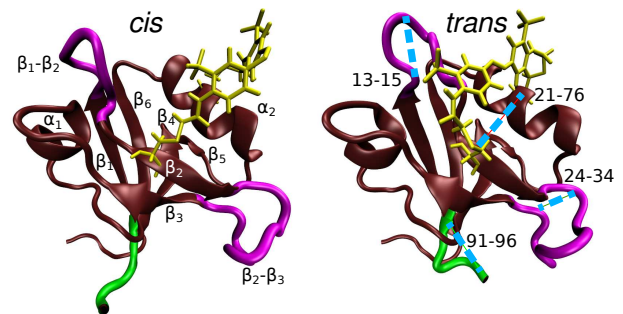


FIG. 1. MD snapshots of PDZ2 in *cis* (left) and *trans* (right) equilibrium states, showing α -helices and β -sheets in brown, loop regions in purple, the C-terminal in green, and the azobenzene photoswitch including linker atoms in yellow. Labels in the left panel indicate the regions β_1 (residues 6–12), β_2 (20–23), β_3 (35–40), α_1 (45–49), β_4 (57–61), β_5 (64–65), α_2 (73–80), and β_6 (84–90). Important loops connecting these regions include β_1 - β_2 (13–19), β_2 - β_3 (24–34), β_3 - α_1 (41–44), and α_2 - β_6 (81–83). The blue lines in the right panel indicate selected $C\alpha$ -distances which characterize the conformational transition following *cis*-*trans* photoisomerization of PDZ2. Adapted with permission from Ref. 32.

II. REAL TIME OBSERVATION OF THE ALLOSTERIC TRANSITION

As a first impression of the time-resolved response of PDZ2 upon photoswitching, Fig. 2a displays results of the transient infrared (IR) experiment of Buchli et al. [31] at selected frequencies ω across the amide I band. Since the corresponding $C=O$ vibrators of the protein backbone are coupled among each other, the amide I band depends, in a rather indirect way, on the structure of the protein [54]. While it is usually not possible to infer detailed structural changes from the transient amide I spectrum, the various timescales of the process can still be determined. To that end, we show cuts of the transient IR difference spectrum and represent the resulting time traces $s_\omega(t)$ on a logarithmic time axis. The logarithmic scale represents an exponential decay with a single decay time τ by a sigmoidal-type shape, i.e., a smoothed step function around τ . Evidently, the time traces $s_\omega(t)$ in Fig. 2a do not exhibit one or a few well-defined decay times. Rather they show a whole spectrum of time scales, covering six decades in time from 10 ps to 10 μ s.

To facilitate a quantitative analysis, we define for each time trace a “dynamical content” $D_\omega(\tau_i)$, which is a probability distribution of the amount of dynamics occurring at timescale τ_i [46–49]. To this end, we perform a fit of $s_\omega(t)$ to a multiexponential response function [Eq. (1)], that assigns to each timescale τ_i a weight (or amplitude), the negative of which is the dynamical content (see Methods for details). Depending on the detection frequency, we can find in Fig. 2a virtually any decay time in the IR spectral response. Moreover, almost all time traces show one or even two “overshootings” of the signal, which in

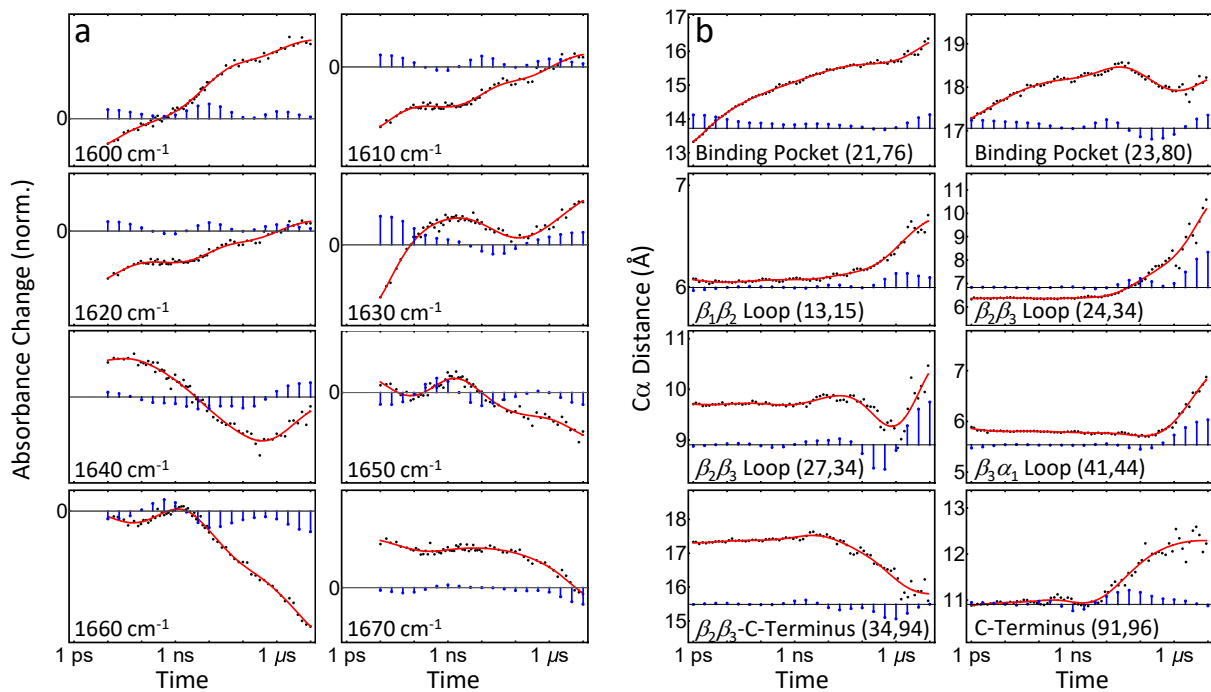


FIG. 2. Time-dependent description of the structural response of a photoswitchable PDZ2 domain, using a logarithmic scale for the time axis. (a) Normalized transient IR time traces (black circles and red fits) across the amide I band in steps of 10 cm⁻¹, which are reproduced from Buchli et al. [31]. Due to limited time resolution, there is no experimental data for the first decade. (b) Time evolution (black circles and red fits) of selected C α -distances of PDZ2, obtained from nonequilibrium MD simulations by Buchenberg et al. [32]. Blue bars indicate the associated dynamical content of experimental and MD data, that is, the weight of time scale τ_i in a multiexponential response function. Adapted with permission from Refs. 31 and 32.

some cases (e.g., for $\omega = 1630$ and 1640 cm⁻¹) are quite prominent.

To comprise the above timescale analysis in a single plot, Fig. 3a shows the “averaged dynamical content” $D(\tau_i)$ [Eq. (2)] of the experimental data. Interestingly, the timescale distribution reveals three well-defined maxima at 10 ps, 10 ns and 10 μ s, with the first and last being at the boundaries of the distribution. It should be mentioned that the 10 ps process probably contains significant contributions from heating of the protein induced by the photoswitching, which is reflected in the IR spectra but does not necessarily affect the structure of the protein on that timescale [55, 56]. The fact that $D(\tau_i)$ still rises at the maximum timescale considered indicates that the process is not quite completed within 10 μ s. On the other hand, the similarity of the transient difference spectrum at 10 μ s with the FTIR difference spectrum seems to suggest that the process is in fact almost completed [31].

To facilitate a direct simulation of the above described time-resolved experiments, Buchenberg et al. [32] performed nonequilibrium MD simulations of the allosteric transition in the PDZ2 domain. By mimicking the initial *cis*→*trans* photoisomerization of the azobenzene photo-switch via a potential-energy surface switching method [57], 100 nonequilibrium trajectories of 1 μ s length were generated, of which 20 randomly selected were extended

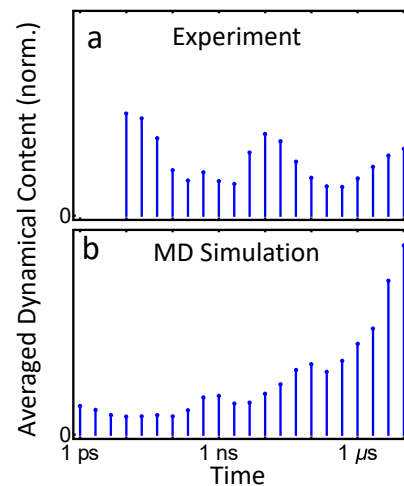


FIG. 3. Averaged dynamical content $D(\tau_i)$ as a function of time constant τ_i , pertaining to (a) all available transient IR time traces from the experimental data [31], and (b) the time evolution of all C α -distances from the MD data [32].

to 10 μ s. Performing an ensemble average to calculate time-dependent observables, photoinduced structural changes of PDZ2 were described in terms of the time evolution of backbone dihedral angles, residue-residue contacts, and C α -distances between residues. To con-

duct a timescale analysis of the nonequilibrium MD data in a similar vein as done for the experimental results, here we focus on the time evolution of C α -distances $d_{i,j}(t)$ between residues i and j .

While a comprehensive collection of C α -distances naturally yields a detailed description of the conformational dynamics, it is instructive to focus on a few representative coordinates that illustrate various important motions associated with the structural transition in PDZ2. Starting from the anchor residues of the photoswitch, the photoinduced structural perturbation is expected to propagate via various intermediate secondary structure segments to the C-terminus, chosen here as an example of a region that is quite remote from the perturbation. On this way, one finds that the relatively rigid α -helices and β -sheets of PDZ2 undergo only small modifications, while the flexible loops of the system, in particular $\beta_1\beta_2$ and $\beta_2\beta_3$, exhibit significant changes of numerous residue-residue contacts and backbone dihedral angles [58]. As representative examples, Fig. 2b shows C α -distances $d_{i,j}(t)$ that reflect the opening of the binding pocket [for $(i, j) = (21, 76)$ and $(23, 80)$] as well as conformational rearrangements of loops $\beta_1\beta_2$ (13,15), $\beta_2\beta_3$ (24,34), (27,34), and $\beta_3\alpha_1$ (41,44). The response of the C-terminus is illustrated by its distance to $\beta_2\beta_3$ (34,94) and its end-to-end distance (91,96). A structural illustration of some of these distances is provided in Fig. 1.

Similar to the experimental results, we find that the MD time traces shown in Fig. 2b cover all timescales, from pico- to microseconds. As maybe expected, we find picosecond dynamics mainly in the observables $d_{21,76}$ and $d_{23,80}$ describing the initial rearrangement around the binding pocket. That fast process, however, is somewhat artificial, as it is induced by the strong force applied by the photoswitch and therefore would not happen in the same way upon ligand binding/unbinding in the native system [59]. (For example, the sheer event of unbinding of a ligand takes on the order of 1 ns already [60].) On the other hand, structural dynamics on nano- and microsecond timescales is observed in all observables. Moreover, the MD time traces exhibit peculiar overshootings, e.g., (27,34), again quite similar to experiment.

Comparing the averaged dynamical content of the MD data (comprising 4650 C α -distances, see Fig. 3b) to experimental findings (Fig. 3a), we notice that the MD results also reveal maxima at the boundaries of the distribution. Because only relatively few C α -distances report on the ps response of the binding pocket, the lower boundary maximum for MD is not very pronounced in the averaged dynamical content. Moreover, we find weak maxima around 1 and 100 ns, which are similar but not identical to the experimental results. Due to the different nature of the observables, IR spectra and C α -distances in fact are expected to represent different projections of the time-dependent structural evolution of the system. While the same timescales are present, the amplitudes of these timescales may therefore be different for experimental and MD data.

As indicated by the experimental averaged dynamical content shown in Fig. 3a, the photoinduced response of PDZ2 appears to occur in three phases which are characterized by timescales of 10 ps, 10 ns and 10 μ s, respectively. Considering the overall similarity of IR and MD time traces with respect to timescales and general features (such as overshootings), in the following we assume that the nonequilibrium MD simulations provide at least a qualitative description of the allosteric transition in PDZ2. This allows us to exploit these simulations in order to develop a microscopic understanding of the underlying dynamical processes. Proceeding this way, Buchenberg et al. [32] identified the three phases of the structural transition as elastic response ($\lesssim 0.1$ ns), inelastic reorganization (~ 100 ns) and structural relaxation ($\gtrsim 1\mu$ s) of PDZ2, which are briefly described in the following.

Accounting for the initial process, the elastic phase describes the photoinduced opening of the binding pocket as described by the C α -distance $d_{21,76}$. As shown in Fig. 2b, the time-dependent average value $d_{21,76}(t)$ increases within 1 μ s by ≈ 0.3 nm, with the first half of the increase occurring within only 0.1 ns. Because this initial expansion of the binding pocket hardly involves conformational transitions including the crossing of free energy barriers, the protein would elastically return to the initial state if the azobenzene switched back to its *cis* configuration. Hence the first phase accounts for the elastic response of the protein. During the first tens of picoseconds, we also observe the dissipation of photoinduced excess kinetic energy, i.e., the cooling of PDZ2 to the solvent temperature [56, 61].

The subsequent expansion of the binding pocket on a nanosecond timescale and the propagation of this conformational change via the adjacent $\beta_1\beta_2$ and $\beta_2\beta_3$ loops, however, require an *inelastic* rearrangement of the protein. As representative observables monitoring this second phase of the protein's response, Fig. 2b shows C α -distances $d_{23,80}$, $d_{13,15}$, $d_{24,34}$ and $d_{27,34}$, which reflect these conformational rearrangements. The overshootings of $d_{23,80}$ and $d_{27,34}$ reflect complex reorganization of the binding pocket and the making and breaking of interresidue contacts, respectively [32]. Eventually, the structural changes of $\beta_1\beta_2$ and $\beta_2\beta_3$ extend via various ways to the distant C-terminal region, e.g., via contacts of $\beta_2\beta_3$ and the C-terminal loop (see the contact formation revealed by $d_{34,94}(t)$). Described by its end-to-end distance, $d_{91,96}$, the response of the C-terminus is seen to be delayed until ~ 10 ns, when $d_{91,96}(t)$ starts to increase on a 100 ns timescale. Hence we find that the inelastic phase begins on a timescale of a few ns and leads to a significant structural reorganization of PDZ2 on a 100 ns timescale.

The qualitative changes of the time evolution of most observables in Fig. 2b for $t \gtrsim 1 \mu$ s indicate a new phase of structural dynamics. This third and final phase of the structural response of PDZ2 is found to describe the *relaxation* of the nonequilibrium conformational distribu-

tion towards the *trans* equilibrium state [32]. Employing density-based clustering [62] of the time-dependent structural distribution, this relaxation process has been shown to occur in a hierarchical way [63–65]. That is, we find that the relatively fast (100 ns) motion of the conformational reorganization in phase 2 represents a prerequisite of the slow (10 μ s) structural relaxation in phase 3.

III. FREE ENERGY LANDSCAPE OF THE ALLOSTERIC TRANSITION

While we have so far explained allosteric communication as a series of local structural changes, it is important to note that these changes do not necessarily occur in a directed sequence as in a falling row of dominoes, except for the fact that everything follows upon the initial 1 ps process around the binding pocket. Beyond that 1 ps process similar timescales are found in Fig. 2b for all observables, regardless whether they are close to or far away from the effector site. For example, the remote C-terminus settles already between ~ 100 ns to 1 μ s (see $d_{91,96}$ and $d_{34,94}$ in Fig. 2b); significantly earlier than the binding pocket itself ($d_{21,76}$ and $d_{23,80}$ in Fig. 2b). Also the ensemble-averaged structural evolution seems to suggest that on all timescales numerous steps happen simultaneously.

To further investigate this notion, we change to a global view of the dynamics and perform a dihedral angle principal component analysis [66, 67] of the *cis* and *trans* equilibrium trajectories. The well-established approach achieves an efficient dimensionality reduction of the high-dimensional atomic motion to a low-dimensional reaction coordinate that subsequently can be used for the interpretation of the considered process [68]. Employing the first two principal components PC1 and PC2 that reflect the largest variance of the protein motion, Fig. 4a shows the resulting *cis* and *trans* free energy landscapes $\Delta G = -k_B T \ln P(\text{PC1}, \text{PC2})$, which can be directly obtained from the probability distribution P along these coordinates. We find that the *cis* and *trans* conformations are well separated along the first principal component, while the second principal component accounts for the conformational heterogeneity of the $\beta_1\beta_2$ and $\beta_2\beta_3$ loops. As a consequence, the latter is important for the description of the structural reorganization of these loops during the second phase of the allosteric transition.

By calculating the probability distribution of all nonequilibrium trajectories, we may also define a free energy landscape associated with the nonequilibrium evolution [32]. Figure 4b shows that this nonequilibrium energy surface overlaps well with the landscapes of the *cis* and *trans* equilibrium states, which suggests that our (up to 10 μ s long) trajectories may be sufficient to cover a considerable part of the overall conformational transition. In the following we adopt this representation to study the behavior of *single* trajectories of the nonequilibrium simulation. Showing the color-coded time evolution of four representative nonequilibrium trajectories

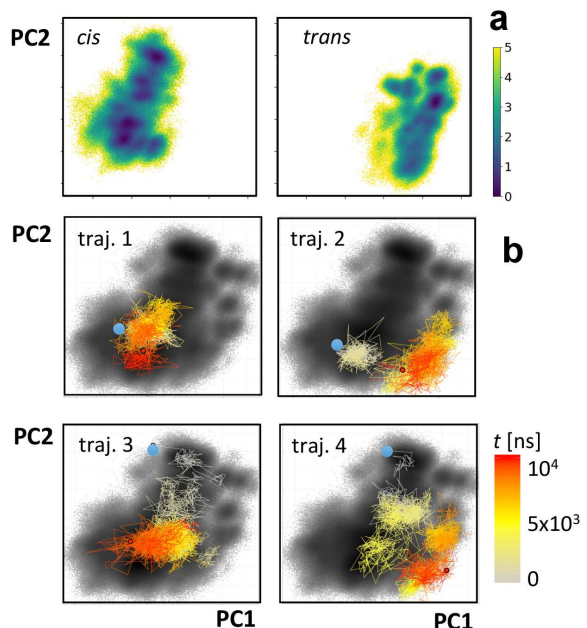


FIG. 4. Two-dimensional representation of the free energy landscape ΔG (in units of $k_B T$), plotted as a function of the first two principal components PC1 and PC2. (a) Energy landscapes associated with the *cis* and *trans* equilibrium states of PDZ2. (b) Free energy landscape associated with the nonequilibrium allosteric transition, drawn as black background. The colored lines indicate the time evolution of selected single nonequilibrium trajectories. Adapted with permission from Ref. 32.

lution of four representative nonequilibrium trajectories in $PC1$ - $PC2$ space, Fig. 4b reveals that all examples are vastly different, indicating a substantial structural diversity of the allosteric transition. Structural analyses show that these changes do not necessarily correspond to a directed sequence of along certain residues, but may also occur *nonlocally*. That is, if a protein contains rather rigid segments (such as the β barrel of PDZ domains), the initially applied conformational stress may directly propagate to distant sites and cause a structural change there. The feasibility of nonlocal and multiple simultaneous structural changes along a single trajectory together with the substantial heterogeneity found for different trajectories clearly suggest that the commonly used term “allosteric pathway” should not be taken literally as in a falling row of dominoes [5, 53].

Another interesting observation from Fig. 4 are the frequent changes and back-crossings of the trajectories between neighboring conformations, which resemble a *diffusive* motion on the free energy landscape, similar as discussed for protein folding [18, 19]. Rather than the conventional picture of two-state folding with a dominant free energy barrier giving rise to single exponential kinetics, the structural rearrangements underlying allosteric communication resembles to a certain extent a ‘down-hill folding’ scenario [16–18, 51, 52]. Proceeding from high-energy unfolded conformations to low-energy native

states without passing major (say, $\gtrsim 3k_B T$) free energy barriers, downhill folders may exhibit numerous significantly populated conformational states that are connected by a large number of transition pathways. This structural and dynamical heterogeneity typically leads to highly nonexponential kinetics, which is what we see in Figs. 2. Just like for proteins that are characterized as downhill-folder [47], the dynamical content of Figs. 2 and 3 contains a continuum of timescales with some substructure, but without any clear gap that would indicate a separation of timescales between the crossing of a dominant barrier and the dynamics within free energy basins. However, different from the protein folding problem, the system first evolves from an ordered initial state into a disordered ensemble, before it again relaxes into a relatively ordered final state, as evidenced by the relatively narrow *cis* and *trans* equilibrium free energy surfaces (Fig. 4a) and the much wider nonequilibrium distribution (Fig. 4b). In this sense, allosteric communication may be considered as an “order-order” transition.

IV. EQUILIBRIUM VS. NONEQUILIBRIUM DESCRIPTION

It is interesting to compare the above nonequilibrium approach to the more common equilibrium description of the structural dynamics associated with the allosteric transition. As prime examples for the latter, NMR experiments as well as MD simulations have observed significant changes of the equilibrium dynamics upon an allosteric transition [1, 2, 69, 70]. These changes have been discussed as a possible driving force of allostery, in particular, in the absence of essential structural changes [21, 22]. The PDZ2 domain is considered as an example in this regard [33]. This rises the question to what extent equilibrium and nonequilibrium descriptions carry the same information on the allosteric transition.

If the protein responds linearly to the perturbation (e.g., caused by ligand binding), the dynamics observed in an equilibrium experiment (such as NMR spectroscopy) should contain the same dynamical content as the dynamics observed in a nonequilibrium experiment (such as pump-probe spectroscopy). This equivalence is a consequence of Onsager’s regression hypothesis [71] which, however, holds only in the case of small nonequilibrium perturbations that explore regions on the free energy surface that are not outside the energy landscape explored in the equilibrium case. In the case of the here studied photoswitchable PDZ2 domain, the linear response assumption may become questionable. First, it is clear from the discussion of Fig. 2 that the mechanical response of the protein (including overshootings etc.) is inelastic, because, e.g., contacts are broken and formed. These findings cannot be described by a harmonic force field (used, e.g., in the popular elastic network models [72, 73]), in which all forces are linear. MD simulations using common biomolecular force fields as well as NMR

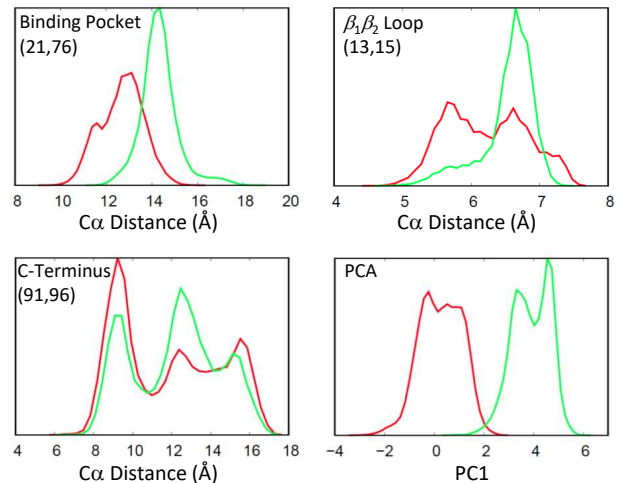


FIG. 5. Different reaction coordinates may discriminate the *cis* (red) and *trans* (green) equilibrium states of PDZ2 differently. Shown are distributions of $C\alpha$ distances (21,76), (13,15) and (91,96) as well as of the first principle component PC1. Adapted with permission from Ref. 32.

experiments, on the other hand, certainly may account for these effects.

It is less clear, though, if the basic assumption of Onsager’s regression hypothesis is appropriate; that is, if the nonequilibrium perturbations explore the same free energy surface than the equilibrium states. This hypothesis is also presumed by the “population shift” model, that explains allostery in terms of a shift of the population probability of various equilibrium states [2]. Employing a principle component analysis, we have shown in Fig. 4a that the free energy surfaces of the *cis* and *trans* equilibrium states hardly overlap, which challenges the idea of a population shift. Of course, the notion of overlapping free energy surfaces depends to a large extend on the reaction coordinates used to represent the energy landscape [74]. This aspect is illustrated in Fig. 5, which compares the distribution of the first principle component (essentially the projection of Fig. 4a onto the PC1 axis) to distributions of selected $C\alpha$ -distances. The distance distributions (which are similar to what an NMR experiment might measure) are seen to strongly overlap for the *cis* and *trans* equilibrium states, even in the case of the distance $d_{21,76}$, on which the photoswitch acts directly. For $d_{13,15}$, and even more so for $d_{91,96}$, the range of possible distances is essentially the same in both states of the protein; just various distances are weighted differently. The overlapping distributions of $C\alpha$ -distances therefore seem to directly support the classical view of a population shift model [2].

The principal component analysis, on the the other hand, maximizes the separation between the two states by including all correlations between structural measures that go into the analysis. From the one-dimensional projection in Fig. 5, the overlap of both distributions is only 6 %, which reduces further to 0.6 % when the overlap

is calculated using the first seven principal components which show structured distributions and slowly decaying autocorrelation functions [32]. Since in fact the effective dimensionality of the dynamical system may be larger than seven [75–78], we expect the true overlap to be even smaller. That is, by employing a reaction coordinate that is able to account for the global conformational rearrangement of the allosteric transition, we find that free energy surfaces of the *cis* and *trans* equilibrium states hardly overlap. Given the limited sampling of equilibrium MD trajectories, however, some asymptotically small overlap of the equilibrium energy landscapes with the full range of the nonequilibrium energy surface can never be ruled out. In that sense, the possible equivalence of visited equilibrium and nonequilibrium phase spaces becomes a somewhat academic and hardly verifiable question.

Looking at it from a different perspective, nonequilibrium experiments and simulations may be considered as an “importance sampling” approach that facilitates an easy exploration of the parts of the energy landscape that account for the allosteric transition. That is, the nonequilibrium simulations cover the full energy landscape (Fig. 4b), while the equilibrium simulations separate the free energy surfaces of the *cis* and *trans* states (Fig. 4a). In the same vein, various nonequilibrium enhanced sampling techniques exist that explore a rarely sampled transition state by mechanically pulling the system towards this direction [79–81]. In that sense, nonequilibrium experiments and simulations are an effective and direct way to study the real time dynamics underlying the allosteric transition. Again, this is similar to the case of protein folding, where pump-probe-type (nonequilibrium) experiments have been designed to effectively study the folding dynamics [24–29].

V. CONCLUDING REMARKS

Combining time-resolved IR spectroscopy and nonequilibrium MD simulations, this joint experimental/computational study has shown that the allosteric transition in PDZ2 amounts to a propagation of conformational change throughout the protein. The associated structural reorganization process is mediated by a change of atomic contacts and dihedral angles in the flexible loop regions of the system. This manifests itself in the transient overshooting of several observables (Fig. 2), which indicate, e.g., that first some contacts need to be broken, before dihedral angles can change and new contacts are formed. In this sense, allosteric communication is a genuinely inelastic and nonlinear process. The nonequilibrium simulations have shown nonlocal and multiple simultaneous structural changes, even along single trajectories. Taken together with the exceeding structural heterogeneity found for different trajectories, we conclude that the notion of “allosteric pathways” should not be taken literally as a directed sequence of structural changes along certain residues.

The time evolution of the allosteric transition in PDZ2 rather resembles a downhill folding scenario, showing diffusive motion on a flat and rugged free energy landscape, which gives rise to a large ensemble of different transition paths. Moreover, we have found that the common assumption of linear response becomes questionable in the case of the photoswitchable PDZ2 domain considered here, which also means that equilibrium and nonequilibrium methods may reveal different aspects of the allosteric system. In any case, we have demonstrated that nonequilibrium experiments and simulations are an effective and appealing way to study dynamical aspects of allostery.

Clearly, further studies are required to reveal if these findings are special for PDZ2 or may be found more generally in other allosteric systems. In particular, the photoswitch in the current model system is quite artificial, and it is therefore not clear *a priori* to what extent it affects the dynamics and the conclusions drawn here. To achieve a less artificial construct, a phototriggerable protein system enabling to initiate ligand-binding/unbinding would be desirable. To this end, a photoswitchable ligand may be designed such that its binding affinity to an allosteric protein changes in the two states of the photoswitch [82]. Ligand unbinding is a unimolecular reaction that does not include any diffusive (slow) step. Therefore it may allow us to investigate the dynamic response of the protein in close analogy to the study of Buchli et al. [31]. Another very interesting construct, that would constitute a truly allosteric system, would be to attach the azobenzene-photoswitch to the C-terminal α -helix of PDZ3, and observe ligand unbinding upon photo-induced unfolding of the helix [30]. That helix has been shown to be allosterically coupled with peptide ligand binding [34]. In addition, site specific vibrational labeling [83, 84] would reveal site-specific information, similar to Fig. 2b from the MD simulation.

VI. METHODS

Following Ref. [46], we define the “dynamical content” $D_j(\tau)$ of a nonequilibrium time trace $s_j(t)$ as the negative of its derivative with respect to the logarithm of time. To calculate $D_j(\tau)$ for the noisy experimental data [31] and MD data [32], we need to first smooth them by fitting to an appropriate function. To that end, we choose a multiexponential response function

$$s_j(t) = a_{0j} + \sum_i a_{ij} e^{-t/\tau_i}, \quad (1)$$

where the time constants τ_i are kept fixed in the fit and distributed equally on a logarithmic scale with 3 terms per decade. The coefficients a_{ij} are the free fit parameters that result in a lifetime spectrum for each time trace $s_j(t)$ as a function of time constant τ_i . As nicely discussed in Ref. [49], the time derivative of each exponential term in Eq. (1), when taken on a logarithmic time-axis, is

reasonably well localized around the corresponding time constant τ_i . Hence the definition of the dynamical content $D_j(\tau_i)$ given in Ref. [46] is equivalent to the negative of the lifetime spectra a_{ij} , i.e., $D_j(\tau_i) = -a_{ij}$.

Fitting Eq. (1) corresponds to an inverse Laplace transformation, which is an ill-posed problem, because the exponential functions in Eq. (1) are not orthogonal to each other [50]. To render the fitting algorithm stable, we therefore introduce a penalty function $\sum_i (a_{ij} - a_{i+1,j})^2$ that enforces a smooth spectrum of coefficients a_{ij} [48] and minimize a weighted sum of this penalty function together with the usual root mean square deviation of the fit function $s_j(t)$ to the data. The weighting factor was determined empirically.

For the “averaged dynamical content” $D(\tau_i)$, we calculate

$$D(\tau_i) = \sqrt{\sum_j a_{ij}^2}, \quad (2)$$

and subsequently normalize it. In Ref. [46], the dynamical content was calculated from equilibrium correlation

functions and hence is always positive (assuming the underlying dynamics is Markovian and diffusive [85]). In the nonequilibrium case considered here, positive and negative values a_{ij} can be obtained, which is why we average the squares of a_{ij} .

Acknowledgments: We thank Brigitte Stucki-Buchli and Steven Waldauer as well as Sebastian Buchenberg, Florian Sittel and Benjamin Lickert for providing the experimental and computational data, respectively, and all of them for numerous important discussions of the project. The work has been supported in part by a European Research Council (ERC) Advanced Investigator Grant (DYNALLO) and by the Swiss National Science Foundation (SNF) through the NCCR MUST and Grant 200021 165789/1 to PH, as well as by Grant STO 247/10 to GS by the Deutsche Forschungsgemeinschaft.

Authors’ contributions: PH together with his research group carried out the experimental work, and GS together with his research group the computational work, on which this Perspective is based. Both authors reanalyzed the data and wrote the manuscript.

-
- [1] D. Kern and E. Zuiderweg, The role of dynamics in allosteric regulation, *Curr. Opin. Struct. Biol.* **13**, 748 (2003).
 - [2] K. Gunasekaran, B. Ma, and R. Nussinov, Is allostery an intrinsic property of all dynamic proteins?, *Proteins* **57**, 433 (2004).
 - [3] Q. Cui and M. Karplus, Allostery and cooperativity revisited, *Protein Science* **17**, 1295 (2008).
 - [4] J.-P. Changeux, Allostery and the Monod-Wyman-Changeux model after 50 years, *Ann. Rev. Biophys.* **41**, 103 (2012).
 - [5] H. N. Motlagh, J. O. Wrabl, J. Li, and V. J. Hilser, The ensemble nature of allostery, *Nature (London)* **508**, 331 (2014).
 - [6] R. Nussinov, Special issue on protein ensembles and allostery, *Chem. Rev.* **116**, 6263 (2016).
 - [7] J. Guo and H.-X. Zhou, Protein allostery and conformational dynamics, *Chem. Rev.* **116**, 6503 (2016).
 - [8] N. V. Dokholyan, Controlling allosteric networks in proteins, *Chem. Rev.* **116**, 6463 (2016).
 - [9] O. Schueler-Furman and S. J. Wodak, Computational approaches to investigating allostery, *Curr. Opin. Struct. Biol.* **41** (2016).
 - [10] S. Brüscheiler, P. Schanda, K. Klobner, B. Brutscher, G. Kontaxis, R. Konrat, and M. Tollinger, Direct observation of the dynamic process underlying allosteric signal transmission, *J. Am. Chem. Soc.* **131**, 3063 (2009).
 - [11] H. S. Chung and W. A. Eaton, Single-molecule fluorescence probes dynamics of barrier crossing, *Nature* **502**, 685 (2013).
 - [12] J. S. Hub, M. Kubitzki, and B. L. de Groot, Spontaneous quaternary and tertiary T-R transitions of human hemoglobin in molecular dynamics simulation, *PLoS Comput. Biol.* **6**, e1000774 (2010).
 - [13] F. Pontiggia, D. Pachov, M. Clarkson, J. Villali, M. Hagan, V. Pande, and D. Kern, Free energy landscape of activation in a signalling protein at atomic resolution, *Nat. Comm.* **6**, 7284 (2015).
 - [14] C. A. Smith, D. Ban, S. Pratihari, K. Giller, M. Paulat, S. Becker, C. Griesinger, D. Lee, and B. L. de Groot, Allosteric switch regulates protein-protein binding through collective motion, *Proc. Natl. Acad. Sci. USA* **113**, 3269 (2016).
 - [15] K. A. Dill, S. Banu Ozkan, M. Scott Shell, and T. R. Weikl, The protein folding problem, *Annu. Rev. Biophys.* **37**, 289 (2008).
 - [16] J. Kubelka, J. Hofrichter, and W. A. Eaton, The protein folding “speed limit”, *Curr. Opin. Struct. Biol.* **14**, 76 (2004).
 - [17] M. Gruebele, Fast protein folding, in *Protein Folding, Misfolding and Aggregation*, pages 106–138, The Royal Society of Chemistry, 2008.
 - [18] J. N. Onuchic, Z. L. Schulten, and P. G. Wolynes, Theory of protein folding: The energy landscape perspective, *Annu. Rev. Phys. Chem.* **48**, 545 (1997).
 - [19] K. A. Dill and H. S. Chan, From Levinthal to pathways to funnels: The “new view” of protein folding kinetics, *Nat. Struct. Bio.* **4**, 10 (1997).
 - [20] G. R. Bowman, V. S. Pande, and F. Noe, *An Introduction to Markov State Models*, Springer, Heidelberg, 2013.
 - [21] A. Cooper and D. Dryden, Allostery without conformational change - a plausible model, *Europ. Biophys. J. Biophys. Lett.* **11**, 103 (1984).
 - [22] T. C. B. McLeish, T. L. Rodgers, and M. R. Wilson, Allostery without conformational change: modelling protein dynamics at multiple scales, *Phys. Biol.* **10**, 056004 (2013).
 - [23] A. H. Zewail, *Femtochemistry: Atomic-Scale Dynamics*

- of the Chemical Bond, *J. Phys. Chem. A* **104**, 5660 (2000).
- [24] P. A. Thompson, W. A. Eaton, and J. Hofrichter, Laser temperature jump study of the helix-coil kinetics of an alanine peptide interpreted with a 'kinetic zipper' model, *Biochemistry* **36**, 9200 (1997).
- [25] K. C. Jones, C. S. Peng, and A. Tokmakoff, Folding of a heterogeneous β -hairpin peptide from temperature-jump 2D IR spectroscopy, *Proc. Natl. Acad. Sci. USA* **110**, 2828 (2013).
- [26] T. P. Causgrove and R. B. Dyer, Nonequilibrium protein folding dynamics: laser induced pH-jump studies of the helix-coil transition, *Chem. Phys.* **323**, 2 (2006).
- [27] M. L. Donten, S. Hassan, A. Popp, J. Halter, K. Hauser, and P. Hamm, pH-jump induced leucine zipper folding beyond the diffusion limit, *J. Phys. Chem. B*, 1425.
- [28] C. Renner and L. Moroder, Azobenzene as conformational switch in model peptides, *Chem. Bio. Chem.* **7**, 869 (2006).
- [29] P. Hamm, J. Helbing, and J. Bredenbeck, Two-dimensional infrared spectroscopy of photoswitchable peptides, *Annu. Rev. Phys. Chem.* **59**, 291 (2008).
- [30] J. A. Ihalainen, B. Paoli, S. Muff, E. H. G. Backus, J. Bredenbeck, G. A. Woolley, and P. Hamm, α -helix folding in the presence of structural constraints, *Proc. Natl. Acad. Sci. USA* **105**, 9588 (2008).
- [31] B. Buchli, S. A. Waldauer, R. Walser, M. L. Donten, R. Pfister, N. Bloechliger, S. Steiner, A. Caffisch, O. Zerbe, and P. Hamm, Kinetic response of a photoperurbed allosteric protein, *Proc. Natl. Acad. Sci. USA* **110**, 11725 (2013).
- [32] S. Buchenberg, F. Sittel, and G. Stock, Time-resolved observation of protein allosteric communication, *Proc. Natl. Acad. Sci. USA* **114**, E6804 (2017).
- [33] E. Fuentes, C. Der, and A. Lee, Ligand-dependent dynamics and intramolecular signaling in a PDZ domain, *J. Mol. Biol.* **335**, 1105 (2004).
- [34] C. M. Petit, J. Zhang, P. J. Sapienza, E. J. Fuentes, and A. L. Lee, Hidden dynamic allostery in a PDZ domain, *Proc. Natl. Acad. Sci. USA* **106**, 18249 (2009).
- [35] H.-J. Lee and J. J. Zheng, PDZ domains and their binding partners: structure, specificity, and modification, *Cell Commun. Signal.* **8** (2010).
- [36] F. Ye and M. Zhang, Structures and target recognition modes of pdz domains: recurring themes and emerging pictures, *Biochem. J.* **455**, 1 (2013).
- [37] S. W. Lockless and R. Ranganathan, Evolutionarily conserved pathways of energetic connectivity in protein families, *Science* **286**, 295 (1999).
- [38] N. Ota and D. A. Agard, Intramolecular signaling pathways revealed by molecular anisotropic thermal diffusion, *J. Mol. Biol.* **351**, 345 (2005).
- [39] Y. Kong and M. Karplus, Signaling pathways of PDZ2 domain: A molecular dynamics interaction correlation analysis, *Proteins* **74**, 145 (2009).
- [40] Z. N. Gerek and S. B. Ozkan, Change in Allosteric Network Affects Binding Affinities of PDZ Domains: Analysis through Perturbation Response Scanning, *PLoS Comput. Biol.* **7** (2011).
- [41] T. Ishikura, Y. Iwata, T. Hatano, and T. Yamato, Energy exchange network of inter-residue interactions within a thermally fluctuating protein molecule: A computational study, *J. Comput. Chem.* **36**, 1709 (2015).
- [42] A. Kumawat and S. Chakrabarty, Hidden electrostatic basis of dynamic allostery in a pdz domain, *Proceedings of the National Academy of Sciences* **114**, E5825 (2017).
- [43] E. J. Fuentes, S. A. Gilmore, R. V. Mauldin, and A. L. Lee, Evaluation of energetic and dynamic coupling networks in a PDZ domain protein, *J. Mol. Biol.* **364**, 337 (2006).
- [44] S. Gianni, T. Walma, A. Arcovito, N. Calosci, A. Bellelli, A. Engstrom, C. Travaglini-Allocatelli, M. Brunori, P. Jemth, and G. W. Vuister, Demonstration of long-range interactions in a PDZ domain by NMR, kinetics, and protein engineering, *Structure* **14**, 1801 (2006).
- [45] J. Zhang, P. J. Sapienza, H. Ke, A. Chang, S. R. Hengel, H. Wang, G. N. Phillips, Jr., and A. L. Lee, Crystallographic and Nuclear Magnetic Resonance Evaluation of the Impact of Peptide Binding to the Second PDZ Domain of Protein Tyrosine Phosphatase 1E, *Biochem.* **49**, 9280 (2010).
- [46] D. E. Shaw et al., Atomic-level characterization of the structural dynamics of proteins, *Science* **330**, 341 (2010).
- [47] K. Lindorff-Larsen, S. Piana, R. O. Dror, and D. E. Shaw, How fast-folding proteins fold, *Science* **334**, 517 (2011).
- [48] J. Joh and J. A. D. Alamo, A current-transient methodology for trap analysis for gan high electron mobility transistors, *IEEE Trans. Electron Devices* **58**, 132 (2011).
- [49] A. Knyazev, Q. Gao, and K. Teo, Multi-exponential lifetime extraction in time-logarithmic scale, in *Advances in Data Mining. Applications and Theoretical Aspects. ICDM 2016. Lecture Notes in Computer Science, Vol 9728*, edited by P. Perner, pages 282–296, Springer, Cham, 2016.
- [50] A. T. N. Kumar, L. Zhu, J. F. Christian, A. A. Demidov, and P. M. Champion, On the Rate Distribution Analysis of Kinetic Data Using the Maximum Entropy Method: Applications to Myoglobin Relaxation on the Nanosecond and Femtosecond Timescales, *J. Phys. Chem. B* **105**, 7847 (2001).
- [51] J. Sabelko, J. Ervin, and M. Gruebele, Observation of strange kinetics in protein folding, *Proc. Natl. Acad. Sci. USA* **96**, 6031 (1999).
- [52] V. Munoz, Conformational dynamics and ensembles in protein folding, *Annu. Rev. Biophys. Biomol. Struct.* **36**, 395 (2007).
- [53] T. McLeish, M. Cann, and T. Rogers, Dynamic Transmission of Protein Allostery without Structural Change: Spatial Pathways or Global Modes?, *Biophysical Journal* **109**, 1240–1250 (2015).
- [54] A. Barth and C. Zscherp, What vibrations tell us about proteins, *Q. Rev. Biophys.* **35**, 369 (2002).
- [55] P. Hamm, S. M. Ohline, and W. Zinth, Vibrational cooling after ultrafast photoisomerization of azobenzene measured by femtosecond infrared spectroscopy, *J. Chem. Phys.* **106**, 519 (1997).
- [56] S. M. Park, P. H. Nguyen, and G. Stock, Molecular dynamics simulation of cooling: Heat transfer from a photoexcited peptide to the solvent, *J. Chem. Phys.* **131**, 184503 (2009).
- [57] P. H. Nguyen and G. Stock, Nonequilibrium molecular dynamics simulation of a photoswitchable peptide, *Chem. Phys.* **323**, 36 (2006).
- [58] S. Buchenberg, V. Knecht, R. Walser, P. Hamm, and G. Stock, Long-range conformational transition in a photoswitchable allosteric protein: A molecular dynamics simulation study, *J. Phys. Chem. B* **118**, 13468 (2014).
- [59] L. Cheng, V. Knecht, and G. Stock, Long-range con-

- formational response of a PDZ domain to ligand binding and release: A molecular dynamics study, *J. Chem. Theo. Comp.* **12**, 870 (2016).
- [60] M. Xu, A. Caflisch, and P. Hamm, Protein Structural Memory Influences Ligand Binding Mode(s) and Unbinding Rates, *J. Chem. Theory Comput.* **12**, 1393 (2016).
- [61] V. Botan, E. Backus, R. Pfister, A. Moretto, M. Crisma, C. Toniolo, P. H. Nguyen, G. Stock, and P. Hamm, Energy transport in peptide helices, *Proc. Natl. Acad. Sci. USA* **104**, 12749 (2007).
- [62] F. Sittel and G. Stock, Robust density-based clustering to identify metastable conformational states of proteins, *J. Chem. Theo. Comp.* **12**, 2426 (2016).
- [63] H. Frauenfelder, S. Sligar, and P. Wolynes, The energy landscapes and motions of proteins, *Science* **254**, 1598 (1991).
- [64] K. A. Henzler-Wildman, M. Lei, V. Thai, S. J. Kerns, M. Karplus, and D. Kern, A hierarchy of timescales in protein dynamics is linked to enzyme catalysis, *Nature (London)* **450**, 913 (2007).
- [65] S. Buchenberg, N. Schaudinnus, and G. Stock, Hierarchical biomolecular dynamics: Picosecond hydrogen bonding regulates microsecond conformational transitions, *J. Chem. Theo. Comp.* **11**, 1330 (2015).
- [66] A. Altis, M. Otten, P. H. Nguyen, R. Hegger, and G. Stock, Construction of the free energy landscape of biomolecules via dihedral angle principal component analysis, *J. Chem. Phys.* **128**, 245102 (2008).
- [67] F. Sittel, T. Filk, and G. Stock, Principal component analysis on a torus: Theory and application to protein dynamics, submitted (2017).
- [68] A. Amadei, A. B. M. Linssen, and H. J. C. Berendsen, Essential dynamics of proteins, *Proteins* **17**, 412 (1993).
- [69] N. Popovych, S. Sun, R. Ebright, and Kalodimos, Dynamically driven protein allostery, *Nat. Struct. Mol. Biol.* **13**, 831 (2006).
- [70] I. Bahar, C. Chennubhotla, and D. Tobi, Intrinsic dynamics of enzymes in the unbound state and relation to allosteric regulation, *Curr. Opin. Struct. Biol.* **17**, 633 (2007).
- [71] D. Chandler, *Introduction to Modern Statistical Mechanics*, Oxford University, Oxford, 1987.
- [72] A. Atilgan, S. Durell, R. Jernigan, M. Demirel, O. Keskink, and I. Bahar, Anisotropy of fluctuation dynamics of proteins with an elastic network model, *Biophys. J.* **80**, 505 (2001).
- [73] C. Chennubhotla and I. Bahar, Signal propagation in proteins and relation to equilibrium fluctuations, *Plos Comput. Biol.* **9**, 1716 (2007).
- [74] R. B. Best and G. Hummer, Reaction coordinates and rates from transition paths, *Proc. Natl. Acad. Sci. USA* **102**, 6732 (2005).
- [75] S. V. Krivov and M. Karplus, Hidden complexity of free energy surfaces for peptide (protein) folding, *Proc. Natl. Acad. Sci. USA* **101**, 14766 (2004).
- [76] T. McLeish, Protein Folding in High-Dimensional Spaces: Hypergutters and the Role of Nonnative Interactions, *Biophysical Journal* **88**, 172–183 (2005).
- [77] R. Hegger, A. Altis, P. H. Nguyen, and G. Stock, How complex is the dynamics of peptide folding?, *Phys. Rev. Lett.* **98**, 028102 (2007).
- [78] S. Piana and A. Laio, Advillin folding takes place on a hypersurface of small dimensionality, *Phys. Rev. Lett.* **101**, 208101 (2008).
- [79] B. Isralewitz, M. Gao, and K. Schulten, Steered molecular dynamics and mechanical functions of proteins, *Current Opinion in Structural Biology* **11**, 224 (2001).
- [80] J. Schlitter, M. Engels, and P. Krüger, Targeted molecular dynamics - a new approach for searching pathways of conformational transitions, *J. Mol. Graph.* **12**, 84 (1994).
- [81] G. Hummer, Nonequilibrium methods for free energy calculations, in *Free Energy Calculations*, edited by C. Chipot and A. Pohorille, pages 171 – 198, Springer, Berlin, 2007.
- [82] S. Kneissl, E. J. Loveridge, C. Williams, M. P. Crump, and R. K. Allemann, Photocontrollable Peptide-Based Switches Target the Anti-Apoptotic Protein Bcl-x_L, *ChemBioChem* **9**, 3046 (2008).
- [83] K. L. Koziol, P. J. M. Johnson, B. Stucki-Buchli, S. A. Waldauer, and P. Hamm, Fast infrared spectroscopy of protein dynamics: advancing sensitivity and selectivity, *Curr. Opin. Struct. Biol.* **34**, 1 (2015).
- [84] P. J. M. Johnson, K. L. Koziol, and P. Hamm, Quantifying Biomolecular Recognition with Site-Specific 2D Infrared Probes, *J. Phys. Chem. Lett.* **8**, 2280 (2017).
- [85] P. Hamm, J. Helbing, and J. Bredenbeck, Stretched versus compressed exponential kinetics in α -helix folding, *Chem. Phys.* **323**, 54 (2006).